Microchim Acta (2012) 178:89–97
DOI 10.1007/s00604-012-0800-y

ORIGINAL PAPER

Magnetic nanoparticles with an imprinted polymer coating for the selective extraction of uranyl ions

Susan Sadeghi · Elias Aboobakri

Received: 7 October 2011 / Accepted: 11 March 2012 / Published online: 20 April 2012

Abstract We have synthesized ferromagnetic nanoparticles with an imprinted polymer coating that is capable of adsorbing and extracting uranyl ions. The adsorbent was characterized using infrared spectroscopy, elemental analysis, X-ray powder diffraction analysis, and scanning electron microscopy. The effects of sample pH, sample volume, weight of the adsorbent, contact time and of other ions have been investigated in the batch extraction mode. The performance of the material was compared to that of particles coated with a non-imprinted polymer. The adsorbent containing the imprinted coating displays higher sorption capacity and better selectivity to uranyl ions. The method was successfully applied to the determination of uranyl ions in water samples.

Keywords Imprinted polymer · Fe_3O_4 magnetic nanoparticles · Extraction · Uranyl ion

Introduction

Solid-phase extraction (SPE) method is being widely utilized for preconcentration and separation of various organic and inorganic analytes prior to analysis for its simplicity, consumption of small volumes of organic solvents and ability to achieve higher enrichment factor[1, 2]. The selectivity of the SPE method has depended on the used adsorbent, so development of new adsorbents with high selectivity, specific recognition and high stability is of great importance [3]. To date, many adsorbents have been employed in SPE of metal ions. An efficient adsorbing material should possess a stable solid support with suitable functional groups for selective interaction with the metal ion. The chelation capability of the functional groups with metal ions is responsible for effectiveness of the adsorbent [4–7]. An approach to improve the selective separation of ions from complex matrix, is utilizing of ion imprinted polymer (IIP) materials as adsorbent [8–12]. The IIPs are generally prepared by polymerization of functional monomers and a cross-linker around a target ion. The subsequent removal of the imprinted ion left behind recognition sites in the polymer which led to the formation of cavities within the polymeric structure. Such cavities are complementary in shape, size and chemical functionality of the imprinted ion that makes it possible to selective rebind to this ion in the presence of other ions [13]. The selectivity of these materials is predominant advantage in separating and analyzing of the imprinted ion from complicated samples and depends on the coordination geometry, coordination number, the charge and size of the imprinted ion [14, 15]. Besides, imprinted polymers are characterized by high chemical and thermal stability as well as good mechanical properties. Comprehensive reviews on imprinted polymers for cations and anions recognition in aqueous media have been published [16–19]. However, due to deeply embedding of the imprinted ion into the IIPs prepared with the conventional imprinting methods, mass transfer of the target ion to the binding sites is low and the obtained recoveries in the SPE processes are poor. Hence, it would be of interest to develop new imprinting methods to overcome these drawbacks. One of the important types of the imprinting methods is surface imprinting; it is based on the surface modification of the matrix materials.

Electronic supplementary material The online version of this article (doi:10.1007/s00604-012-0800-y) contains supplementary material, which is available to authorized users.

S. Sadeghi (✉) · E. Aboobakri
Department of Chemistry, Faculty of Science, University of Birjand,
P.O.Box: 97175/615, Birjand, Iran
e-mail: ssadeghi@birjand.ac.ir

This method is simple and convenient producing imprinted polymers with high selective binding sites and fast binding kinetics [20–29]. To separating the imprinted polymeric adsorbents from the aqueous solution, it is necessary post processing such as filtration and centrifugation that are time consuming. Therefore, the improvement of imprinted polymeric adsorbents for efficient removing of ions and easy collecting the adsorbent from aqueous solutions is of particularly significant.

In recent decade, magnetic nanoparticles, especially Fe_3O_4, have attracted because of its outstanding properties including superparamagnetism and low toxicity. It has potential to apply in various fields including separation and purification [30–32]. In the past few years, new composite materials based on magnetite nanoparticles in which these particles are encapsulated with organic polymers through monomer polymerization or coated with inorganic materials such as silica and titanium dioxides through a sol–gel approach have been widely utilized for extraction and separation of transition metal ions [23, 33–36]. These adsorbents not only have the advantage of magnetism property that provides easily and quickly collecting the adsorbent, but also combination with the properties of imprinted polymers make them as potential materials for selective extraction of the target ions.

Uranium is usually present in natural waters at nanogram per milliliter levels [37, 38] and this extreme dilution in the presence of high concentration of other ions makes it difficult for extraction and direct determination. In this paper, the synthesis of uranyl-imprinted amino functionalized silica coated Fe_3O_4 magnetic nanoparticles as a new adsorbent for uranyl ions extraction is reported. The adsorbent was synthesized by surface imprinting method combined with a sol–gel process without partitioning chelating agent. Characterizations of the new adsorbent were performed by means of scanning electron microscopy (SEM), powder X-ray diffraction (XRD) and Fourier transform infrared (FT-IR) spectroscopy and described in details. Besides to optimize various parameters affecting the adsorption of uranyl ions on the adsorbent, the selectivity of the adsorbent to some inorganic ions was also investigated. The applicability of the developed adsorbent for recovery of uranyl ions in spiked ground water and mineral water samples has been also explored.

Experimental

Equipments

The UV–Vis spectra were recorded on a PC spectrophotometer from Shimadzu model 2501 (Kyoto, Japan, www.shimadzu.com). The FTIR spectra (400–4,000 cm^{-1} were recorded using KBr pellets by VERTEX 70 FT-IR spectrophotometer (Bruker, www.brukeroptics.com). A Shimadzu flame atomic absorption spectrophotometer model AA-6300 was used for determination of transition metals. The X-ray diffraction (XRD) patterns of the Fe_3O_4 nanoparticles and the functionalized Fe_3O_4 nanoparticles were obtained using the Bruker, D8 ADVANCE X-ray diffractometer (Bruker, Germany, www.bruker-axs.com) with Cu Kα source. The 2θ angles were probed from 10° to 80°. A JEOL JSM 6700F scanning electron microscope (Tokyo, Japan, www.jeol.com) was used to study the morphology and shape of the particles of the synthesized ion-imprinted polymer materials. The pH measurements were conducted by a corning 125 pH meter. Deionized water was obtained from an AquaMax system (Anyang, Korea, www.Younglin.com).

Reagents

Reagent grade of uranyl nitrate, $UO_2(NO_3)_2$, $6H_2O$, were obtained from Fluka (Seelze, Germany, www.Fluka.com). Trisodium citrate (99 %) was obtained from Sigma-Aldrich Chemie GmBH (Steinheim, Germany, www.sigmaaldrich.com). $FeCl_2{\cdot}4H_2O$,$FeCl_3{\cdot}6H_2O$, ammonium hydroxide (25 %), 3-aminopropyl triethoxysilane (APS) and tetraethyl orthosilicate (TEOS) were purchased from Merck (Darmstadt, Germany, www.merck.es). All other reagents and solvents used were of the analytical reagent grade and provided from Merck.

Preparation of uranyl-imprinted silica coated magnetic nanoparticles (IIP-SMNP)

Silica coated magnetic nanoparticles were prepared according to the described methods in electronic supplementary material (ESM). To prepare the uranyl-imprinted amino-functionalized silica coated Fe_3O_4 nanoparticles (IIP-SMNP), 0.57 mmol of uranyl nitrate was dissolved in ethanol under stirring and then 0.5 mL of APS was added into the mixture. The solution was stirred for 1 h, to which 0.5 g silica coated Fe_3O_4 nanoparticles in ethanol was added and sonicated for 10 min. After 12 h of stirring at 40 °C, the product was recovered by an external magnetic field, washed with ethyl acetate and ethanol, respectively, to remove the remnant APS. Finally it was washed with 0.1 M EDTA solution for complete removal of uranyl ions from the imprinted polymer. The resulting product was washed with doubly distilled water and ethanol and dried under vacuum at 50 °C for 12 h. For comparative purpose, the non-imprinted functionalized silica coated Fe_3O_4 nanoparticles (NIP-SMNP) was also prepared using an identical procedure in the absence of uranyl ions. The synthesis of the IIP-SMNP via a multistep procedure is illustrated in Fig. 1.

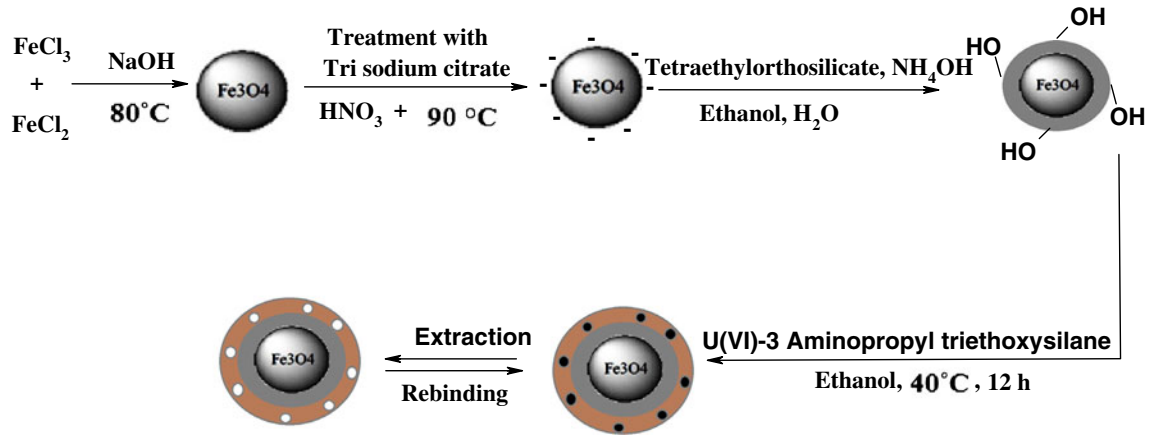

Fig. 1 Schematic of the synthesis steps of uranyl-imprinted functionalized silica coated Fe_3O_4 magnetic nanoparticles (IIP-SMNP)

General procedure for extraction of uranyl ion in batch mode

20 mL solution containing appropriate concentration of uranyl ions was taken and the pH was adjusted to the desired value with 0.01 mol L^{-1} acetate buffer. The solution was transferred to the polyethylene bottles and the adsorbent was added. The mixture was shaken vigorously for appropriate time. Afterwards, the adsorbent was isolated from the solution by an external magnetic field and the equilibrium concentration of uranyl ions in the supernatant (C_e) was determined spectrophotometrically using ArsenazoIII reagent [39]. The percentage of extraction, %E, was calculated by using the following equation:

$$\%E = \frac{C_i - C_e}{C_i} \times 100 \quad (1)$$

where C_i and C_e represent the initial and equilibrium concentrations of uranyl ions in μ mol L^{-1}.

Results and discussion

Preparation of the adsorbent

Fe_3O_4 magnetic nanoparticles were prepared based on the co-precipitation of $FeCl_2$ and $FeCl_3$ upon addition of aqueous NaOH solution. Then, the product was treated with an excess of trisodium citrate solution to obtain the stable magnetite nanoparticles. The modified Fe_3O_4 nanoparticles were easily coated by silica via the well-known Stöber process [40] in which silica was formed in situ through the hydrolysis and condensation of tetraethyl orthosilicate (TEOS). The amino end group of APS can interact with the uranyl ions and then it was grafted onto the surface of silica coated Fe_3O_4 nanoparticles. Thus, uranyl imprinted sol–gel material was obtained by incorporation of uranyl ions into the inorganic silica gel host. The final step was releasing of uranyl ions from the produced polymeric material by using EDTA solution.

Characterization

The structural property of the synthesized polymeric adsorbent based on magnetic nanoparticles was analyzed by X-ray powder diffraction (XRD). XRD patterns of the synthesized Fe_3O_4 nanoparticles in the 2θ region of 10–80° (Fig. S1, ESM) displayed diffraction lines at 2θ: 30.28, 35.41, 43.25, 57.26 and 62.84. These lines are characteristics for spinel structure of Fe_3O_4. From the Scherer equation [41], sizes of the prepared Fe_3O_4 nanoparticles were estimated in the range of 10–17 nm. The XRD patterns of silica coated Fe_3O_4 nanoparticles and uranyl imprinted polymer silica coated Fe_3O_4 particles displayed the same diffraction lines, especially the most intense one at 2θ =35.41°, confirming the presence of the crystalline structure of the magnetite. But, the intensity of the peaks decreased and became wide indicating that coating of nonmagnetic silica shell and imprinted polymer on the surface of Fe_3O_4 nanoparticles have been occurred (Fig. S1).

To know whether imprinted polymer successfully coated on the surface of Fe_3O_4, FT-IR was employed (Fig. S2, ESM). The FT-IR spectrum of Fe_3O_4 nanoparticles showed two absorption peaks at 576.76 and 3400.38 cm^{-1} which are attributed to the Fe-O and OH stretching vibration frequencies. Compared with the untreated magnetite nanoparticles, two new absorption peaks at 1,590 and 1,394 cm^{-1} appeared in the FT-IR spectrum of citrate-treated magnetite nanoparticles, which are assigned to vibration frequencies of carboxyl group. It verified the interaction between the citrate groups and iron ions on the Fe_3O_4 nanoparticles surfaces. The silica coated magnetic nanoparticles also showed a broad band at 1,000–1,260 cm^{-1} and a weak band at 965 cm^{-1} that are relevant to the stretching vibrations of

SiO–Si and Si–OH, respectively. Amino functionalized silica coated magnetic nanoparticles showed the stretching vibrations of OH groups at 3,200 cm^{-1} that overlapped with the stretching vibration of the N–H band, so the infrared spectrum was not conclusive but it could be supported by elemental chemical analysis. According to the microanalysis results (Table S1, ESM), the increase in carbon content and the presence of nitrogen after treatment of silica coated Fe_3O_4 nanoparticles with APS indicated that the attachment of amino groups on the surface of the silica coated magnetic nanoparticles have been occurred.

The surface characterization of the silica coated magnetic nanoparticles and IIP-SMNP were carried out using scanning electron microscopy (SEM) (Fig. 2). Comparison of the SEM image of silica coated magnetic nanoparticles (Fig. 2a) with the IIP-SMNP particles image (Fig. 2b), indicated that in the silica coated magnetic nanoparticles no inter-particle aggregation observed whereas image of the IIP-SMNP showed an aggregation of nanoparticles due to coating of polymer onto the silica coated magnetic nanoparticles surfaces. It revealed that the surface morphology of silica coated magnetic nanoparticles is affected by the polymer grafting process.

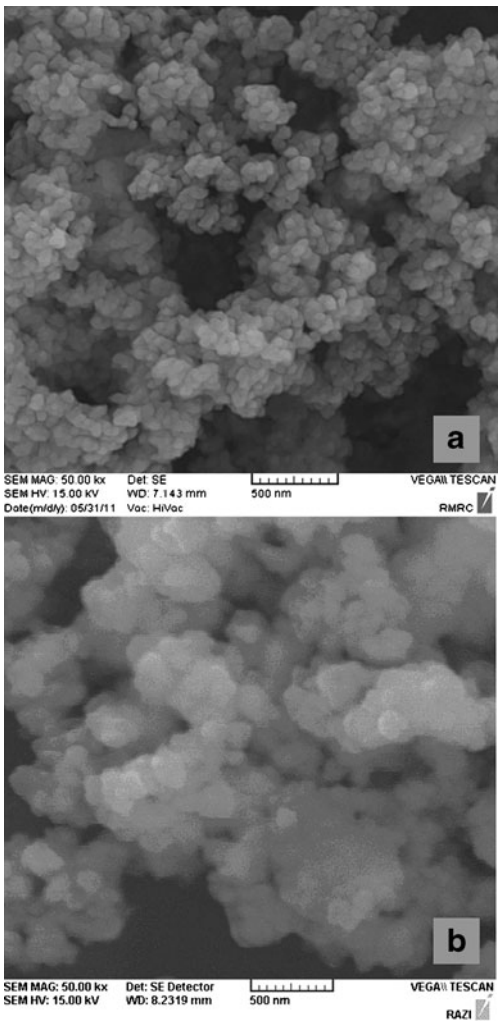

Fig. 2 Scanning electron micrographs of the **a**) silica coated Fe_3O_4 magnetic nanoparticles and **b**) IIP-SMNP

Uranyl extraction studies in batch mode

To find the optimum pH value of sample, 20 mL of solutions containing 10 μmol L^{-1} of uranyl ion in the pH range of 2.0–6.0 were subjected to 10 mg of the IIP-SMNP for 30 min. The results showed that the most extraction of uranyl ions was occurred at pH 4 (Fig. 3). At higher pH values, the extraction efficiency decreased owing to formation of UO_2OH^+ and $(UO_2)_2(OH)_2$ as a results of the hydrolysis of uranyl ions. At strong acidic medium, the extraction efficiency of uranyl ions decreased which may be ascribed to the protonation of amine in the IIP-SMNP adsorbent and decreasing its binding capability. The NIP-SMNP has capability to extract the uranyl ions resulting from the interaction of uranyl ions with amine moiety that randomly distributed all over the matrix of the polymer without any structural arrangement. This can led to non-specific binding sites in the NIP-SMNP for uranyl ions with low affinity. At pH 4, the difference between the extraction efficiency of uranyl ions on IIP-SMNP and NIP-SMNP adsorbents is indicating to more specific interactions of IIP-SMNP with uranyl ions at this pH.

The time effect is an important factor that needs to be considered for optimization. In order to find a right contact time on the extraction efficiency, various experiments were carried out using 20 mL solutions containing 10 μmol L^{-1} uranyl ions at pH 4 subjected to 20 mg adsorbent over a series of shaking time (5–120 min). Figure S3 (ESM) indicates that the time required to achieve the adsorption equilibrium is only 30 min, and there is no obvious change from 30 min to 120 min. The results suggest the IIP-SMNP has small mass-transfer resistance, so that the IIP-SMNP can

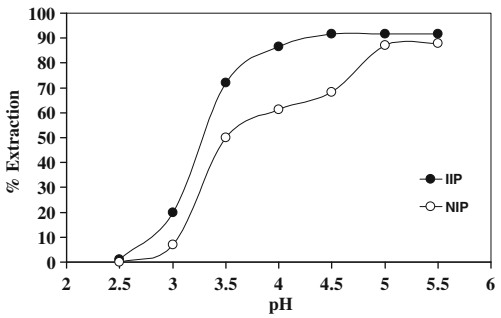

Fig. 3 Influence of pH on the extraction of uranyl ions (experimental conditions; 20 mL of 10 μmol L^{-1} uranyl ions; 10 mg adsorbent; 30 min contact time)

achieve adsorptive equilibrium in a relative short time for uranyl ions.

Effects of the amount of adsorbent (5–50 mg) and the sample volume (10–100 mL) on the extraction of 10 μmol L^{-1} uranyl ions were investigated. The results were expressed in terms of ratio of the weight of the adsorbent to the sample volume (Fig. S4, ESM). It is obvious the extraction efficiency increased as the amount of the adsorbent was increased but the non specific interactions also increased. Thus, 20 mg of the IIP-SMNP was used for quantitative adsorption of uranyl ions in 40 mL solution.

Capacity of the adsorbent

To find the sorption capacity of the adsorbent, aliquots of 20 mL of uranyl ion solutions at various concentrations (5–250 μmol L^{-1}) at pH 4 were equilibrated with 20 mg of the IIP-SMNP and NIP-SMNP for 30 min. The sorption capacity (q_e, mmol g^{-1}) was calculated by Eq. (2) as:

$$q_e = \frac{(C_i - C_e)}{w} v \quad (2)$$

where C_i and C_e are the initial and equilibrium concentrations of uranyl ions (μmol L^{-1}), w is the amount of the adsorbent (g) and v is the volume of the uranyl solution (L). From the plot of q_e versus C_e, the maximum adsorption capacities of the IIP-SMNP and NIP-SMNP adsorbents for uranyl ions were calculated as 25.8 and 9.7 μmol g^{-1}, respectively (Fig. 4). The capacity of the imprinted polymer is higher than that of the non-imprinted polymer. This observation supports that ion imprinting creating specific binding sites within the polymeric matrix that increased affinity of the IIP-SMNP toward the uranyl ions.

The adsorption isotherm was used to evaluate the adsorption properties of the adsorbent in the batch extraction mode at room temperature, which is important for understanding the mechanism of the adsorption. The Langmuir and the Freundlich models were often employed to study the adsorption isotherm of the adsorbent [42, 43].

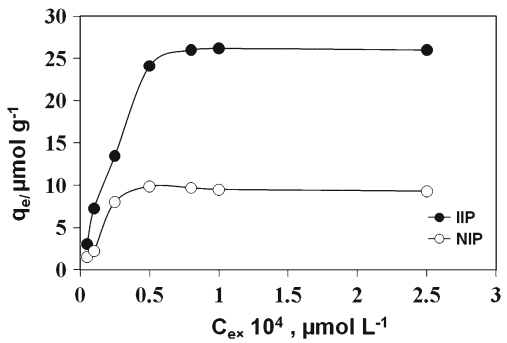

Fig. 4 Adsorption isotherm of uranyl ions on IIP-SMNP (experimental conditions; 20 mg adsorbent; 30 min, 20 mL uranyl ion solutions at various U(VI) concentrations at pH=4)

Langmuir isotherm describes monolayer adsorption based on the assumption that all the adsorption sites have equal adsorbate affinity and also indicates that adsorption at one site does not affect at an adjacent site. The linear form of the Langmuir isotherm is given as Eq. (3):

$$\frac{1}{q_e} = \frac{1}{q_{max} b C_e} + \frac{1}{q_{max}} \quad (3)$$

where q_e describes the amount of uranyl ions adsorbed on the unit amount of the adsorbent at equilibrium (μmol g^{-1}), q_{max} is the maximum adsorption capacity (μmol g^{-1}), C_e is the equilibrium concentration of uranyl ions in the solution (μmol L^{-1}), and b is the Langmuir constant (L μmol^{-1}). q_{max} and b are the Langmuir constants, which can be calculated from the intercept and slope of the linear plot based on $1/q_e$ versus $1/C_e$. In compare to the Langmuir isotherm, Freundlich isotherm model considers the heterogeneous surface adsorption which is based on the energy of the adsorption sites. The linear form of Freundlich isotherm can be written as Eq. (4):

$$\log q_e = \log K_F + \frac{1}{n} \log C_e \quad (4)$$

where K_F is the Freundlich constant and 1/n is the heterogeneity factor. Both K_F and n constants can be calculated from the slope and intercept of the linear plot of log q_e vs. log C_e. The obtained experimental equilibrium data were fitted with Langmuir and Freundlich isotherm models (Fig. S5, ESM) and the results are summarized in Table 1.

The values of the correlation coefficient (R^2) of the linear plots of Langmuir and Freundlich isotherms showed that the Langmuir adsorption model was fitted better to the experimental results. Moreover, the calculated value of q_{max} (30.03 μmol g^{-1}) from Langmuir equation was very close to the experimental value of 25.8 μmol g^{-1}. This implies that the surface imprinted particles possess almost homogeneous adsorption sites and good mass transfer facilitating diffusion of uranyl ions to the active binding sites. The possible reason for lower the experimental q_{max} value than that of the theoretical might be embedment a small fraction of binding sites in the polymeric matrix in the imprinting

Table 1 The Langmuir and Freundlich isotherm parameters for sorption of uranyl ions by IIP-SMNP adsorbent

Langmuir model			Freundlich model		
q_{max} (μmol g^{-1})	b (L μmol^{-1})	R^2	K_F (μmol g^{-1})	n	R^2
30.03	0.7655	0.9950	8.0556	2.7956	0.9209

process which were not accessible by the uranyl ions. The high value of b (0.7655) is relevant to strong attraction of uranyl ions on the adsorbent surface.

Adsorption kinetics

The kinetics of adsorption of uranyl ions on the IIP-SMNP adsorbent was investigated to find the controlling mechanism of adsorption process. Three kinetic models i.e. Lagergren pseudo first order, pseudo second order and Weber-Morris intra-particle diffusion models were chosen. The kinetics of adsorption normally include two stages; a rapid removal stage followed by a slower stage before the equilibrium approaches.

The pseudo first order kinetic model expressed as Eq. (5):

$$\log(q_e - q_t) = \log q_e - 0.434K_f \quad (5)$$

Where q_t and q_e are the amounts of ion adsorbed at time t and at equilibrium (μmol g^{-1}), respectively, and k_f is the rate constant of pseudo first order adsorption process (min^{-1}). From the slope and intercept of the plot of log (q_e–q_t) versus t, the first order rate constant and equilibrium adsorption capacity pseudo can be determined.

Pseudo second order kinetic model describes the reversibility of equilibrium between liquid and solid phase and is expressed as the following Eq (6):

$$t/q_t = 1/\left(K_s q_e^2\right) + t/q_e \quad (6)$$

where K_s is the second order rate constant (g μmol^{-1} min^{-1}). The plot of t/q_t versus t gives a linear relationship and K_s and q_e can be determined from the slope and intercept of the line, respectively.

In a rapidly stirred batch sorption, the intra-particle diffusion may be the controlling factor in determining the kinetics of the process. This kinetic model is presented by Eq. (7):

$$q_t = K_{id}t^{0.5} + C \quad (7)$$

where K_{id} is the intra-particle diffusion rate constant (μmol g^{-1} $min^{-0.5}$) and C is a constant (μmol g^{-1}). If the plot of q_t versus $t^{0.5}$ gives a straight line, then the sorption process is only controlled by intra-particle diffusion, otherwise two or more steps influence on the sorption process. The plot showed that the data points related by two straight lines. Such deviation of straight line from the origin indicates that the pore diffusion is not the only rate-controlling step. The kinetic rate constants, q_e and correlation coefficients (R^2) of the linear plots of the kinetic models are summarized in Table S2 (ESM). According to these results, the kinetic data are well described on pseudo second order that provided the best correlation coefficient and agreement between the calculated and experimental values of q_e. The K_s rate constant calculated from the slope of the linear plot via Eq. (6) was 0.048 g μmol^{-1} min^{-1} and suggests that chemisorption may be the rate-determining step in the adsorption process. However, the rate controlling mechanism may interchangeably vary in multiple possible manners during the course of the adsorption process.

Effect of interfering ions

The effect of potentially interfering ions on the sorption of uranyl ions was also studied. To investigate the interference effect of these ions (Table 2), binary solutions containing 10 μmol L^{-1} of the uranyl ions and the various interference-to- uranyl molar ratios were subjected to the batch extraction mode. The reported tolerance limit is defined as the ion concentration causing a relative error <±5 % in the extraction percentage of uranyl ions. The results are summarized in Table 2. As can be seen, the presence of major ions has no significant influence on the determination of uranyl ions under the selected conditions. This indicates that the binding sites have higher affinity toward uranyl ions over the possible interfering ions.

The effect of ionic strength on the extraction efficiency of uranyl ions using NaCl and KCl salts at 0.02 mol L^{-1} and $MgCl_2$ and $CaCl_2$ at 0.01 mol L^{-1} concentrations have also been investigated. The results showed that in the presence of 1,000 fold or more of potassium, sodium, magnesium and calcium ions, the extraction efficiency of uranyl ions had no significant change and suggested that this adsorbent would be suitable for extraction of uranyl ions from relatively high saline solutions.

Selectivity of the imprinted adsorbent

To find an estimation of selectivity of IIP-SMNP and NIP-SMNP to uranyl ions, the selectivity coefficients of these adsorbents toward uranyl ions with respect to the competing cations i.e. Fe^{3+}, La^{3+}, Ce^{3+}, Zr^{4+} and Th^{4+} were evaluated. These competitive ions were probed because of similar

Table 2 Tolerance limits of some cations on the adsorption of uranyl ions[a] onto the IIP-SMNP at optimum conditions

Foreign ion	Tolerance limit (mole ratio)
Na^+, K^+	2000
Mg^{2+}, Ca^{2+}	1000
Mn^{2+}, Zn^{2+}, Co^{2+}, Ni^{2+}, Cd^{2+}, Pb^{2+}	200
Cu^{2+}	80

[a] 20 mL of 10 μmol L^{-1} uranyl ion solution under optimal experimental conditions

chemical behaviors with UO_2^{2+} ions and often coexisting in their minerals. Effects of competitive ions on the extraction of uranyl ions were evaluated by the distribution ratio (k_d) and selectivity coefficient values of IIP-SMNP and NIP-SMNP. Distribution ratio of the adsorbent, k_d, towards the metal ions was calculated by Eq. (8):

$$K_d = \frac{(C_i - C_e)}{C_e} \times \frac{v}{w} \quad (8)$$

Selectivity coefficient for uranyl ion relative to interfere ions (K) is defined as Eq. (9):

$$K = \frac{K_d{}^{UO_2{}^{2+}}}{K_d{}^{M^{n+}}} \quad (9)$$

where $K_d{}^{UO_2{}^{2+}}$ and $K_d{}^{M^{n+}}$ are distribution ratios of uranyl and interfere ions, respectively. The K_d and K values of Fe^{3+}, La^{3+}, Ce^{3+}, Zr^{4+} and Th^{4+} with respect to UO_2^{2+} ions are summarized in Table 3. As it is expected, except for Th^{4+}, the ability binding of IIP-SMNP to uranyl ions is stronger than that for Fe^{3+}, La^{3+}, Ce^{3+}, Zr^{4+} ions. The high binding ability of Th^{4+} to the IIP-SMNP might be due to the nearly identical size but higher charge of thorium than uranyl ion.

Analytical performance

The limit of detection of the method, as the concentration equivalent to three times of standard deviation of the blank divided into the slope of the calibration curve, was 0.027 μmol L^{-1} (7.32 μg L^{-1}) uranyl ions. The relative standard deviation (RSD) for five replicate extractions of 10 μmol L^{-1} uranyl ions was 2.1 % indicating that the method exhibited good precision for the analysis of uranyl ions in aqueous solutions. The sorption capacity of the synthesized adsorbent stored at ambient conditions did not change during 3 months.

Table 3 Distribution ratio (K_d) and selectivity coefficient (K) values of IIP-SMNP

Cation	[a]Hydrated ionic radius (Å)	K_d	$K = \frac{K_d{}^{UO_2{}^{2+}}}{K_d{}^{M^{n+}}}$
UO_2^{2+}	0.89	31924	–
Th^{4+}	0.94	12638	2.5
Zr^{4+}	0.74	2968	10.8
La^{3+}	1.03	134	238.5
Ce^{3+}	1.01	283	112.8
Fe^{3+}	0.65	1731	18.5

[a] Shannon R D (1976) Acta Crystallographica. A32: 751–767

Application

The applicability of the IIP-SMNP for extraction of trace level concentration of uranyl ions in real matrices, two water samples ground water (Shokat Abad Ganat, Birjand, Iran) and mineral water samples (Damavand spring, Damavand, Iran) were analyzed. Before the analysis, the samples were filtered through a 45 μm membrane filter. For the extraction procedure, pH of 40 mL of the water samples was adjusted to 4.0 and spiked with 0.074 μmol L^{-1} uranyl ions and was subjected to the adsorbent. The adsorbed uranyl ions were estimated based on triplicate analysis (Table 4). The results clearly indicate that the adsorbent was successfully applied to the quantitative extraction of the trace uranyl ions even in the presence of various diverse ions in real water samples.

Conclusions

In this study, a new uranyl-imprinted material was prepared by surface modification of silica coated Fe_3O_4 magnetic nanoparticles for selective extraction of uranyl ions. The prepared adsorbent showed high affinity and fast kinetics process for uranyl ions. The kinetics and mechanism for adsorption of uranyl ions on the imprinted polymer followed the second order rate kinetics and Langmuir adsorption isotherm, respectively. The IIP-SMNP had higher adsorption capacity for uranyl ions than NIP-SMNP, and the method was successfully applied to the analysis of trace uranyl ions in aqueous solution. The precision and accuracy of the method was satisfactory. This work provides a platform to prepare ion imprinted polymer functionalized magnetic nanoparticles with high affinity, selectivity and capacity to nearly any target ions.

Table 4 Recoveries of uranyl ions spiked in water samples[a] by IIP-SMNP adsorbent

Sample	Amount of added(μg L^{-1})	% Recovery[b]
Underground water	0	–
	20	89.90±2.1
Mineral water[c]	0	–
	20	93.02 ±3.5

[a] 0.074 μmol L^{-1} (20 μg L^{-1}) U(VI) ions spiked in 40 mL water samples

[b] Average of three replicates±S.D

[c] The composition of mineral water sample (mg/L): Ca^{2+} 56.4, Mg^{2+} 15.4, Na^+ 4.6, K^+ 0.6, HCO_3^- 212, F^- 0.2, Cl^- 6, SO_4^{2-} 10.6, NO_3^- 7.5, NH_4^+ 0.1

Acknowledgments The authors gratefully acknowledge the support of this work by the Birjand University Research Council.

References

1. Hennion MC (1999) Solid-phase extraction: method development, sorbents, and coupling with liquid chromatography. J Chromatogr A 856:3–24
2. Fontanals N, Marcé RM, Borrull F (2005) New hydrophilic materials for solid-phase extraction. TrAC, Trends Anal Chem 24:394–406
3. Thuman EM, Mills MS (1998) Solid phase extraction, in: Principles and Practice. Wiley, New York
4. Pyrzyñska K, Trojanowicz M (1999) Functionalized cellulose sorbents for preconcentration of trace metals in environmental analysis. Crit Rev Anal Chem 29:313–321
5. Jal PK, Patel S, Mishra BK (2004) Chemical modification of silica surface by immobilization of functional groups for extractive concentration of metal ions. Talanta 62:1005–1028
6. Matoso E, Kubota LT, Cadore S (2003) Use of silica gel chemically modified with zirconium phosphate for preconcentration and determination of lead and copper by flame atomic absorption spectrometry. Talanta 60:1105–1111
7. Goswami A, Singh AK (2002) 1,8-Dihydroxyanthraquinone anchored on silica gel: synthesis and application as solid phase extractant for lead(II), zinc(II) and cadmium(II) prior to their determination by flame atomic absorption spectrometry. Talanta 58:669–678
8. Sadeghi S, Akbarzadeh Mofrad A (2007) Synthesis of a new ion imprinted polymer material for separation and preconcentration of traces of uranyl ions. React Funct Polym 67:966–976
9. Esen C, Andac M, Bereli N, Say R, Henden E, Denizli A (2009) Highly selective ion-imprinted particles for solid-phase extraction of Pb2+ ions. Mater Sci Eng C 29:2464–2470
10. Ng S-M, Narayanaswamy R (2010) Demonstration of a simple, economical and practical technique utilizing an imprinted polymer for metal ion sensing. Microchim Acta 169:303–311
11. Kloskowski A, Pilarczyk M, Przyjazny A, Namieśnik J (2009) Progress in development of molecularly imprinted polymers as sorbents for sample preparation. Crit Rev Anal Chem 39:43–58
12. Leśniewska B, Kosińska M, Godlewska-Żyłkiewicz B, Zambrzycka E, Wilczewska AZ (2011) Selective solid phase extraction of platinum on an ion imprinted polymers for its electrothermal atomic absorption spectrometric determination in environmental samples. Microchim Acta 175:273–282
13. Sellergren B (2001) Molecular imprinted polymers, 1st edn. Elsevier, Netherlands
14. Kabanov VA, Efendiev AA, Orujev DD (1979) Complex-forming polymeric sorbents with macromolecular arrangement favorable for ion sorption. J Appl Polym Sci 24:259–267
15. Shirvani-Arani S, Ahmadi SJ, Bahrami-Samani A, Ghannadi-Maragheh M (2008) Synthesis of nano-pore samarium(III)-imprinted polymer for preconcentrative separation of samarium ions from other lanthanide ions via solid phase extraction. Anal Chim Acta 623:82–88
16. Mosbach K (1994) Molecular imprinting. Trends Biochem Sci 19:9–14
17. Ewen SL, Steinke JHG (2008) Molecularly imprinted polymers using anions as templates. Struct Bond 129:207–248
18. Wu X (2012) Molecular imprinting for anion recognition in aqueous media. Microchim Acta 176:23–47
19. Prasada Rao T, Kala R, Daniel S (2006) Metal ion-imprinted polymers-Novel materials for selective of recognition inorganics. Anal Chim Acta 578:105–116
20. Tsukagoshi K, Yu KY, Maeda M, Takagi M (1993) Metal ion-selective adsorbent prepared by surface- Imprinting polymerization. Bull Chem Soc Jpn 66:114–120
21. He Q, Chang XJ, Wu Q, Huang XP, Hu Z, Zhai YH (2007) Synthesis and applications of surface-grafted Th(IV)-imprinted polymers for selective solid-phase extraction of thorium(IV). Anal Chim Acta 605:192
22. Gao BJ, An FQ, Zhu Y (2007) Novel surface ionic imprinting materials prepared via couple grafting of polymer and ionic imprinting on surfaces of silica gel particles. Polymer 48:2288–2297
23. Quirarte-Escalante CA, Soto V, De La Cruz W, Porras GR, Manríquez R, Gomez-Salazar S (2009) Synthesis of hybrid adsorbents combining sol–gel processing and molecular imprinting applied to lead removal from aqueous streams. Chem Mater 21:1439–1450
24. Chang XJ, Jiang N, Zheng H, He Q, Hu Z, Zhai YH et al (2007) Solid-phase extraction of iron(III) with an ion-imprinted functionalized silica gel sorbent prepared by a surface imprinting technique. Talanta 71:38
25. Liu Y, Liu Z, Wang Y, Dai J, Gao J, Xie J et al (2011) A surface ion-imprinted mesoporous sorbent for separation and determination of Pb(II) ion by flame atomic absorption spectrometry. Microchim Acta 172:309–317
26. Cheng Z, Wang H, Wang H, He F, Zhang H, Yang S (2011) Synthesis and characterization of an ion-imprinted polymer for selective solid phase extraction of thorium(IV). Microchim Acta 173:423–431
27. Zheng H, Zhang D, Wang W et al (2007) Highly selective determination of palladium(II) after preconcentration using Pd(II)-imprinted functionalized silica gel sorbent prepared by a surface imprinting technique. Microchim Acta 157:7–11
28. Bi X, Lau RJ, Yang K (2007) Preparation of ion-imprinted silica gels functionalized with glycine, diglycine, and triglycine and their adsorption properties for copper ions. Langmuir 23:8079–8086
29. Mirsky VM, Hirsch T, Piletsky SA, Wolfbeis OS (1999) A spreader-bar approach to molecular architecture: formation of stable artificial chemoreceptors. Angew Chem Int Ed 38:1108–1110
30. Bystrzejewski M, Pyrzyńska K (2011) Kinetics of copper ions sorption onto activated carbon, carbon nanotubes and carbon-encapsulated magnetic nanoparticles. Colloid Surf A: Physicochem Engin Asp 377:402–408
31. Buschow KHJ. Handbook of magnetic materials (2006) Elsevier, Vol. 16, Chapter 5: Synthesis, properties and biomedical applications of magnetic nanoparticles, pp 403–482.
32. Jang JH, Lim HB (2010) Characterization and analytical application of surface modified magnetic nanoparticles. Microchem J 94:148–158
33. Guiying J, Wei L, Shaoning Y, Youyuan P, Jilie K (2008) Novel superparamagnetic core-shell molecular imprinting microspheres towards high selective sensing. Analyst 133:1367
34. Ren YM, Zhang ML, Zhao D (2008) Synthesis and properties of magnetic Cu (II) ion imprinted composite adsorbent for selective removal of copper. Desalination 228:135–149
35. Huang C, Hu B (2008) Silica-coated magnetic nanoparticles modified with γ-mercaptopropyltrimethoxy- silane for fast and selective solid phase extraction of trace amounts of Cd, Cu, Hg, and Pb in environmental and biological samples prior to their determination by inductively coupled plasma mass spectrometry. Spectrochim Acta B 63:437–444
36. Peng H, Wang S, Hu B (2011) Fast and selective magnetic solid phase extraction of trace Cd, Mn and Pb in environmental and biological samples and their determination by ICP-MS. Microchim Acta 175:121–128
37. Prasada Rao T, Metilda P, Gladias JM (2006) Preconcentration techniques for uranium(VI) and thorium(IV) prior to analytical determination: an overview. Talanta 68:1047–1064
38. World Health Organization (1998) Guidelines for drinking water quality, 2nd edition WHO Health Criteria and other supporting information, vol 2. WHO/EOS/98.1, Geneva, p 283
39. Sadeghi S, Shykhzadeh E (2008) Solid phase extraction using silica gel functionalized with Sulfasalazine for preconcentration

of uranium (VI) ions from water samples. Microchim Acta 163:313–320. doi:10.1007/s00604-008-0020-7
40. Stöber W, Fink A, Bohn E (1968) Controlled growth of monodispers silica spheres in the micron size range. J Colloid Interface Sci 26:62–69
41. Burton AW, Ong K, Rea T, Chan IY (2009) On the estimation of average crystallite size of zeolites from the Scherrer equation:A critical evaluation of its application to zeolites with one-dimensional pore systems. Micropor Mesopor Mater 117:75–90
42. Freundlich HMF (1906) Under die adsorption in lösungen. Z Phys Chem 57:385–470
43. Temkin MJ, Pyzhev V (1940) Recent modifications to Langmuir isotherms. Acta Physiochim USSR 12:217–222